DOI: 10.1002/chem.200501484

Surfactant-Assisted Hollowing of Cu Nanoparticles Involving Halide-Induced Corrosion–Oxidation Processes

Chih-Chia Huang,[a] Jih Ru Hwu,[b] Wu-Chou Su,[c] Dar-Bin Shieh,[d] Yonhua Tzeng,[e] and Chen-Sheng Yeh*[a]

Abstract: We have demonstrated a simple fabrication of hollow nanoparticles by halide-induced corrosion oxidation with the aid of surfactants. Cuprous oxide Cu_2O nanoshells can be generated by simply mixing Cu nanoparticles with alkyltrimethylammonium halides at 55 °C for 16 min. The hollowing mechanism proposed is that absorption of surfactants onto the Cu surface facilitates the formation of the void interior through an oxidative etching process. Upon extending the reaction up to 4 h, fragmentation, oxidation, and self-assembly were observed and the CuO ellipsoidal structures were formed. The headgroup lengths of the surfactants influenced the degree of CuO ellipsoidal formation, whereby longer surfactants favored the generation of ellipsoids. Optical absorption measured by UV-visible spectroscopy was used to monitor both oxidation courses of $Cu \rightarrow Cu_2O$ and $Cu_2O \rightarrow CuO$ and to determine the band-gap energies as 2.4 eV for Cu_2O nanoshells and 1.89 eV for CuO ellipsoids. For the contact-angle measurements, the wettability changed from hydrophilicity (18°) to hydrophobicity (140°) as the Cu_2O nanoshells shifted to CuO ellipsoids.

Keywords: copper · corrosion oxidation · halides · nanoshells · self-assembly

Introduction

Copper is an important material because of its high electrical and thermal conductivities. Cu_2O and CuO are known as p-type semiconductors exhibiting narrow band gaps and have been widely used as powerful heterogeneous catalysts.[1,2] For example, Cu_2O has a direct band gap (2 eV), which makes it a promising material for the conversion of solar energy into electrical and chemical energy.[3] Nanoscale materials in various forms, such as one-dimensional, prism, core-shell, and interior hollow structures, are ideally suited for a wide range of applications in science and industry because of their unique optical, magnetic, and catalytic behaviors.

Hollow nanostructures have attracted tremendous interest, due to their potential use in chemical reactors, drug delivery, catalysis, and sensors.[4] Generally, manipulation of hollow materials is performed by depositing the target precursors onto a template, subsequently a calcination or dissolution by using solvents is employed to remove the template.[5] Well-known physical phenomena involving the Kirkendall effect[6] and Ostwald ripening[7] have been introduced successfully to synthesize core-free nanomaterials. Recently, we reported a new form of Au_3Cu_1 alloy-based nanoshells, produced by the reaction of Cu nanoparticles with $HAuCl_4$ on the basis of the differential reduction potentials between $AuCl_4^-/Au$ and Cu^{2+}/Cu (Cu^+/Cu).[8] Here, we demonstrate a new synthetic strategy that can generate hollow nanostructures by a halide-induced corrosion oxidation and with alkyltrimethylammonium halide surfactants. The Cu_2O nanoshells were synthesized by simply mixing Cu colloids with surfactants (CTAX, X = Br^-, Cl^-) at 55 °C

[a] C.-C. Huang, Prof. C.-S. Yeh
Department of Chemistry and Center for Micro/Nano Technology Research
National Cheng Kung University, Tainan 701 (Taiwan)
Fax: (+886) 6-274-0552
E-mail: csyeh@mail.ncku.edu.tw

[b] Prof. J. R. Hwu
Department of Chemistry, National Tsing Hwa University
Hsinchu 300 (Taiwan)

[c] Prof. W.-C. Su
Department of Internal Medicine, National Cheng Kung University
Tainan 701 (Taiwan)

[d] Prof. D.-B. Shieh
Institute of Oral Medicine and Department of Stomatology
National Cheng Kung University, Tainan 701 (Taiwan)

[e] Prof. Y. Tzeng
Department of Electrical Engineering and Center for Micro/Nano Technology Research
National Cheng Kung University, Tainan 701 (Taiwan)

through an oxidative etching process. As the reaction was prolonged, the Cu_2O nanoshells collapsed, oxidized, and assembled into three-dimensional CuO ellipsoids. The formation mechanism is presented as $Cu_{(nanoparticle)} \rightarrow Cu_2O_{(hollow)} \rightarrow CuO_{(ellipsoid)}$. The band gaps ($E_g$) and the wettability were also determined for both Cu_2O nanoshell and CuO ellipsoid nanomaterials.

Results and Discussion

Polydispersed Cu nanoparticles were prepared by laser ablation. The transmission electron microscope (TEM) image (Figure 1) displays the morphology prior to the addition of the cetyltrimethylammonium bromide (C_{16}TAB)/H_2O mixture. The resulting Cu colloidal solution had a deep wine-red color and exhibited particle size distribution of 45.9 ± 19.8 nm.

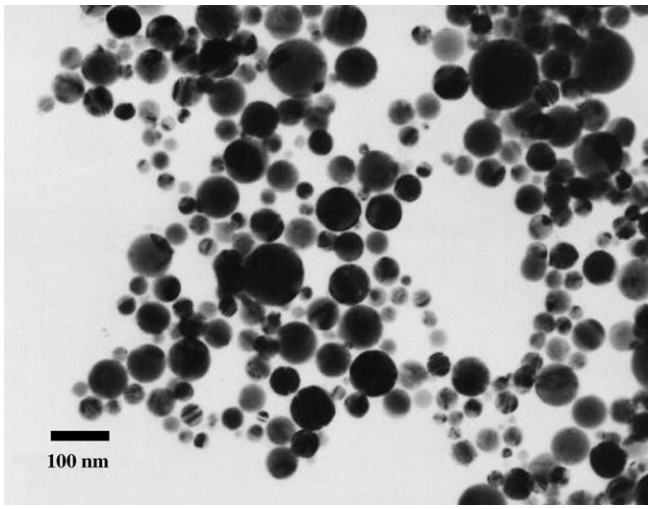

Figure 1. TEM image of the Cu nanoparticles prepared by laser ablation.

After injecting 1 mL of Cu colloidal solution into C_{16}TAB aqueous solution, colloidal copper was gradually oxidized to Cu_2O and CuO at 55 °C. The solution color changed to dark green after 1 min, then turned to pale yellow after 16 min reaction time, indicating the formation of the Cu_2O colloids. The resulting colloids were found to remain as Cu_2O for at least two weeks in air. If the reaction time was prolonged to 4 h, the colloidal solution became orange, indicating CuO formation. The TEM images show that Cu_2O exhibited a hollow structure (Figure 2a) and CuO formed in an ellipsoidal shape (Figure 2b). A single CuO nanoleaf is displayed in the right panel of Figure 2b and the corresponding electron diffraction (ED) pattern indicates that the longitudinal axis [010] is perpendicular to the *c* direction.

The image in Figure 3a shows a single Cu_2O nanoparticle exhibiting light interior contrast compared to the dark periphery, which suggests a core-free nanostructure. It is known that laser ablation readily generates an inhomogeneous distribution in particle size. Interestingly, we found that the hollowing degree is related to particle size. As seen from Figure 3a–d, the hollowing process can be completed more readily in the smaller particles within the same reaction period.

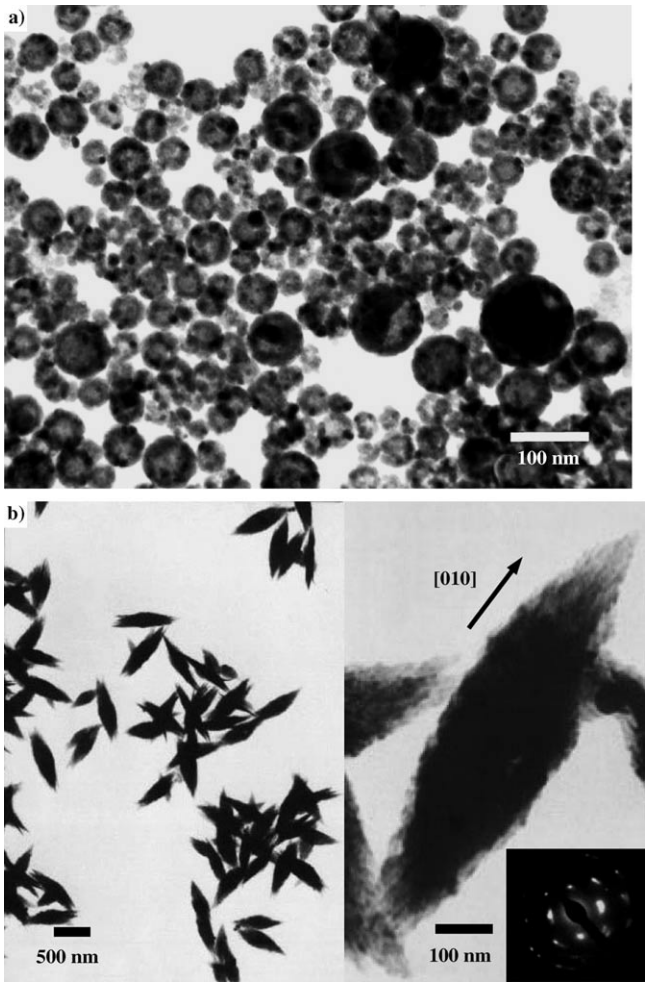

Figure 2. TEM images of 1 mL of colloidal copper injected into 4 mL aqueous solution containing 2.2 mM CTAB at 55 °C for a) 16 min and b) 4 h. The right-hand panel of (b) shows a single CuO ellipsoidal shape and the inset ED pattern was obtained along the [001] zone-axis.

X-ray diffraction (XRD) patterns provide evidence for the structure conversion, as seen in Figure 4. Initially, the laser-ablated colloidal solution exhibited pure Cu nanoparticles, which is consistent with our previous studies.[8,9] After injection of C_{16}TAB, Cu_2O composition increased accompanied with the Cu structure at 10 min. As the reaction was prolonged to 2 h, Cu completely converted to Cu_2O and CuO. Further extension of the reaction up to 4 h resulted in CuO as the final product.

The oxidation reactions resulted in a color change of the colloidal solution: wine red→pale yellow→orange. The optical absorption measured by UV-visible spectrometry was used to monitor the oxidation course: $Cu \rightarrow Cu_2O \rightarrow CuO$. Figure 5a shows the UV-visible evolution in the early stage of the reaction period from Cu nanoparticles to Cu_2O nano-

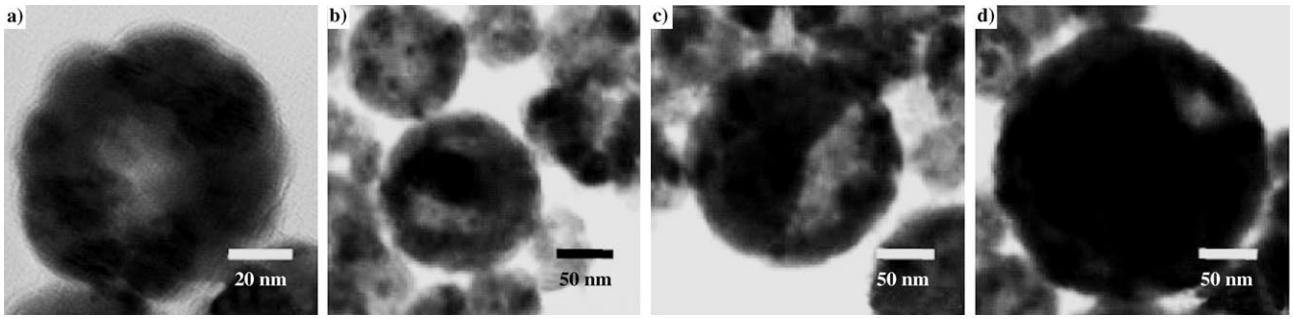

Figure 3. TEM images showing the relationship of hollowing degree to particle size. Particle diameters increase from a) to d). All of the images were taken at the reaction time of 16 min.

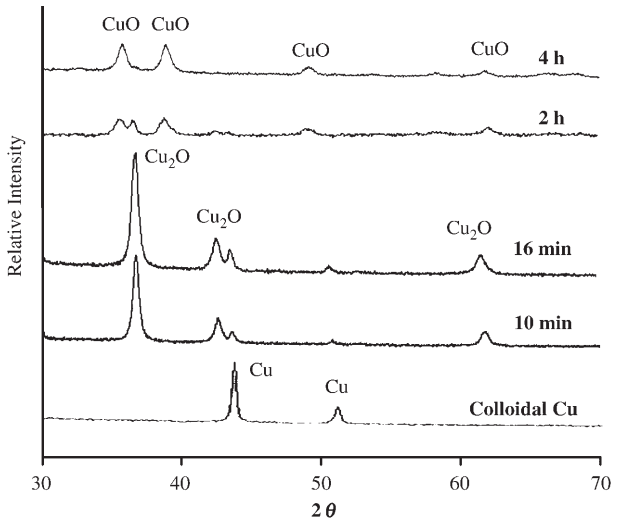

Figure 4. Evolution of XRD patterns as a function of reaction time.

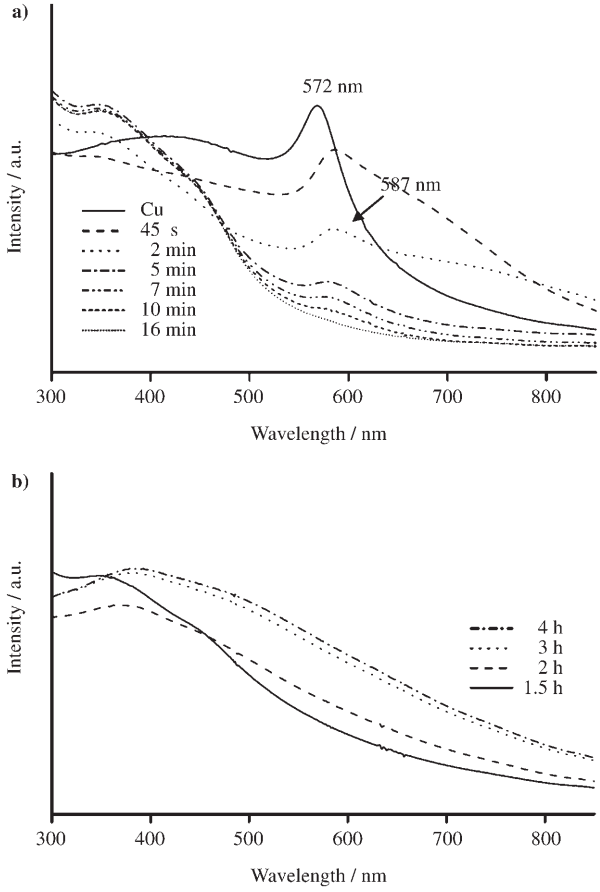

Figure 5. UV-visible absorption spectra obtained over different reaction periods: a) from 45 s to 16 min ($Cu_{nanoparticles} \rightarrow Cu_2O_{nanoshells}$) and b) from 1.5 h to 4 h ($Cu_2O_{nanoshells} \rightarrow CuO_{ellipsoids}$).

shells. The pure Cu colloidal solution has maximum absorption at 572 nm. As the oxidation reaction continued, the absorption band gradually shifted to red (~587 nm) and the intensity decreased until it disappeared after 16 min. This suggests the formation of copper oxide through Cu oxidation.[10] The increased intensity at 360 nm, which is attributed to the band-to-band transition, indicates the presence of Cu_2O.[11,12] As the oxidation reaction was extended up to 4 h, the UV-visible behavior changed, as shown in Figure 5b, and implies that the colloidal nature shifted to another phase.

Figure 6 shows the absorption band-gap E_g values of the Cu_2O hollow spheres and CuO ellipsoids calculated from the absorption curves at 16 min (Figure 5a) and at 4 h (Figure 5b) by using the following equation: $(\alpha h\nu)^n = B(h\nu - E_g)$.[13] The term $h\nu$ represents the photoenergy, α is the absorption coefficient, B is a constant related to the material, and n has a value of either 2 for a direct transition or 1/2 for an indirect transition. The optical band gaps are the extrapolated values at $\alpha = 0$ from the plot of $(\alpha E_{photon})^2$ versus E_{photon}, and give the absorption-edge energies of $E_g =$ 2.46 and 1.89 eV for Cu_2O and CuO, respectively.

The TEM images (Figures 1–3) and XRD results show that the formation process of the Cu-based colloids is $Cu_{(nanoparticle)} \rightarrow Cu_2O_{(hollow)} \rightarrow CuO_{(ellipsoid)}$. Scheme 1 illustrates the hollowing of the particles and the formation of the ellipsoidal structure. The oxide layer formed within the particle periphery after a short reaction time, for example, 45 s, and was accompanied by the formation of the partial interior void. Figure 7a shows the TEM image obtained at 45 s of a single particle displaying partial hollowing. The Cu_2O layer with light contrast developed on the particle surface, as indi-

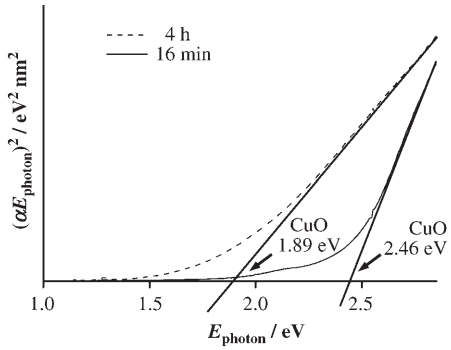

Figure 6. Plot of $(\alpha E_{photon})^2$ vs E_{photon} for Cu_2O nanoshells and CuO ellipsoids.

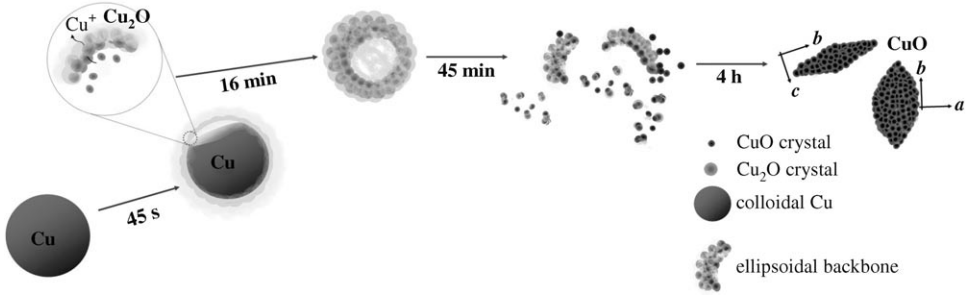

Scheme 1. The oxidative etching and the assembly of the ellipsoidal structures.

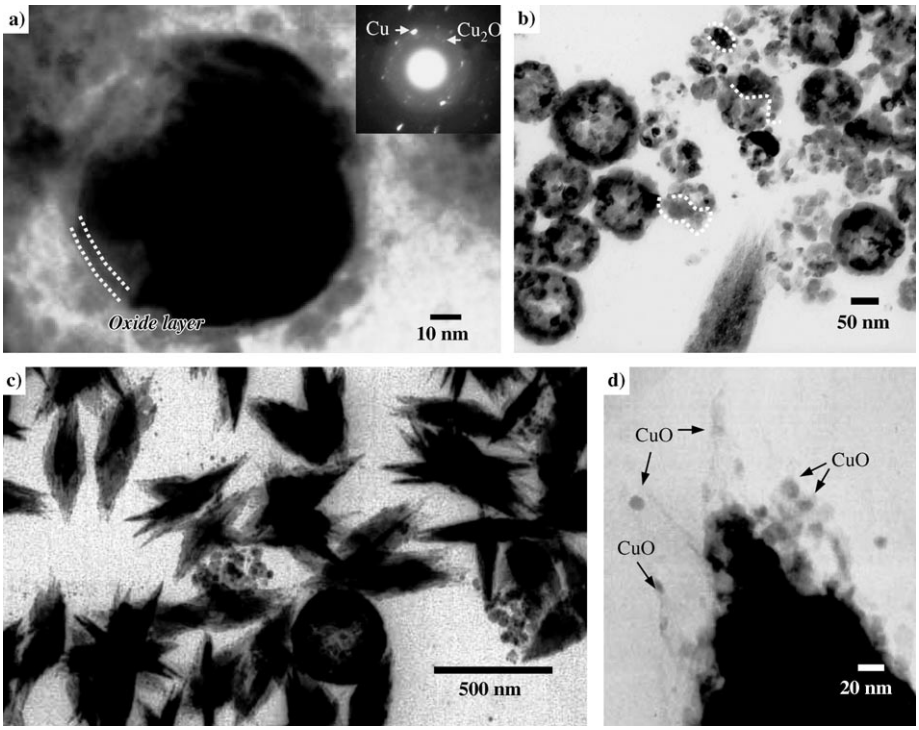

Figure 7. Typical TEM images showing the copper oxidation reaction over different time periods: a) 45 s, b) 45 min, and c,d) 2 h. The inset of (a) is the selected area diffraction pattern for the corresponding particles.

cated by the dotted lines (Figure 7a), and the particle interior showing a dark contrast is composed of Cu. The inset of Figure 7a displays the corresponding selected area electron diffraction patterns, which show both Cu and Cu_2O rings. As the reaction was prolonged, the hollowing process proceeded through the etching of Cu. The consumption of the Cu component is also supported by the UV-visible absorption data shown in Figure 4a, in which the characteristic Cu band completely disappeared after the reaction time of 16 min. As the reaction period was prolonged to 45 min, the Cu_2O hollow nanospheres began to collapse and yielded the spherical particles and islandlike fragments, as indicated by the arrows and dotted lines in Figure 7b. These islandlike fragments are made of many small nanoparticles and are likely to act as ellipsoid backbones for the further development of the CuO ellipsoidal structures (Figure 7c). The higher-resolution image in Figure 7d shows the small CuO nanoparticles assembled into an ellipsoidal morphology. The XRD pattern (obtained after 4 h) in Figure 4 calculated by using the Debye–Scherra equation indicates the crystal domain size of 6.1 nm for CuO.

We have demonstrated the one pot synthesis of hollow Cu_2O nanoshells and ellipsoidal CuO nanostructures through the oxidation, hollowing, fragmentation, and assembly processes. It should be noted that C_{16}TAB was introduced into the reactions. In the absence of C_{16}TAB, no hollow structures were observed for Cu colloids in 2-propanol/H_2O after heating for 10 min at 55 °C. The addition of C_{16}TAB surfactant facilitated solid evacuation in Cu nanospheres. It is known that halide ions play the critical role in both the oxidation and corrosion processes.[14–16] A control experiment involving C_{18}TAC (octadecyltrimethylammonium chloride) surfactant with chloride ions was conducted and yielded the same results, with the formation of both hollow and ellipsoidal structures.

On the basis of Elsner et al.,[16] oxidation of Cu in the presence of halide ions can be described in the following four steps. Initially, both Cu dissolu-

tion and formation of the CuX salt layer occurred simultaneously on the copper surface.

$$Cu+X^- \rightarrow (CuX)_{ad.}+e^- \quad (1)$$

$$Cu+X^- \rightarrow Cu(X)_{ad.}+e^- \quad (2)$$

Steps (3) and (4) followed steps (1) and (2) successively and yielded $Cu(OH)_{ad.}$ and $(Cu_2O)_{ad.}$ following the absorption of water by copper.

$$Cu(X)_{ad.}+H_2O \rightarrow Cu(OH)_{ad.}+(CuX)_{ad.}+H^++e^- \quad (3)$$

$$Cu(OH)_{ad.} \rightarrow (Cu_2O)_{ad.}+H_2O \quad (4)$$

The parenthesis refer to adsorbed species or products (ad.) at the Cu surface in the reactions (1)–(4). Thus, it can be understood that the Cu_2O product was formed in the reaction of Cu colloids with an aqueous solution containing halide ions. In addition to Cu_2O formation, we also identified a hollowing process in this study. In this aspect, the surfactants (CTAX, $X=Br^-$, Cl^-) could have played a role in facilitating the formation of the void interior. For example, the positively charged C_{16}TAB adsorbed electrostatically by means of the headgroup $^+N(CH_3)_3(C_{16}H_{33})$ onto the Cu surface. We measured the ζ-potential of the nascent Cu colloids immediately after laser ablation as -17 mV. Adsorption of the positively charged headgroup could have synchronized with the copper surface oxidation. With the surfactant adsorption, the spherical morphology was maintained in the course of the reaction and the Cu dissolution caused the etching process inside the Cu core. A control experiment was performed by replacing CTAX ($X=Br^-$, Cl^-) with NaBr and this led to the production of many spherical-like Cu_2O particles with very little core-free morphology. Clearly, the carbon chain headgroups affect the formation of the hollow structure in the copper corrosion–oxidation reaction. Notably, Liz-Marzán et al. studied recently the oxidation of Au nanoparticles in the presence of CTAB.[17] $AuCl_4^-$ ions complexed with CTAB led to $AuCl_2^-$ formation by dissolution and oxidation of Au nanoparticles. The similar redox reaction cannot be ruled out and might also take place between Cu nanoparticles and Cu^{2+}–CTAB, resulting in Cu^+ formation to yield Cu_2O.

As shown in Scheme 1, further extension of the reaction time resulted in the collapse of the Cu_2O nanoshells, which fragmented into islandlike domains accompanied by small spherical particles. At this stage, Cu_2O structures started to grow into monoclinic CuO products. Subsequently, these CuO units aggregated and assembled into the ellipsoidal structures. The electron diffraction image (Figure 2b) indicates that these CuO ellipsoids grew in the [010] direction (*b* axis). As measured by XRD, these ellipsoidal structures are assembled from the small CuO nanoparticles with domain size of 6.1 nm. The CuO ellipsoidal structure with the aggregation-based growth of small nanoparticles in a preferred [010] direction, as well as an almost single crystalline diffraction from the aggregated particles are consistent with the previous results from the reaction of Cu foil with formamide through a copper-complexation process.[18] However, the driving force for the morphological transition of the sphere–ellipsoid from cubic Cu_2O to monoclinic CuO remains to be resolved.

Furthermore, we found that surfactants also affected the formation of the final CuO ellipsoidal products. The variation in the headgroup lengths in surfactants, that is, C_{18}TAB, C_{14}TAB, and C_{10}TAB, resulted in different degrees of CuO ellipsoidal formation. Addition of C_{18}TAB yielded the same ellipsoidal products as those with C_{16}TAB (Figure 8a). However, C_{14}TAB yielded only some CuO ellipsoids (Figure 8b), and C_{10}TAB led to hollow nanospheres only (Figure 8c). It seems that the longer headgroup favors ellipsoidal formation, although the detailed mechanism of this remains to be discovered.

Finally, we also investigated the wettability of these oxide nanomaterials. It is known that antifogging and self-cleaning properties are associated with the hydrophilic and hydrophobic natures, respectively, of the material surface. Superhydrophilicity with a contact angle close to 0° and a superhydrophobic surface with a contact angle larger than 150° have attracted great interest because of various applications in industry.[19] The wettability was investigated by measuring the water contact angle. Figure 9a shows an image of the water droplet spread out on the surface of the Cu_2O nanoshells with a water contact angle of 18°. Conversely, a spherical water droplet on the CuO ellipsoidal surface resulted in a contact angle of 140° (Figure 9b). We observed that wetta-

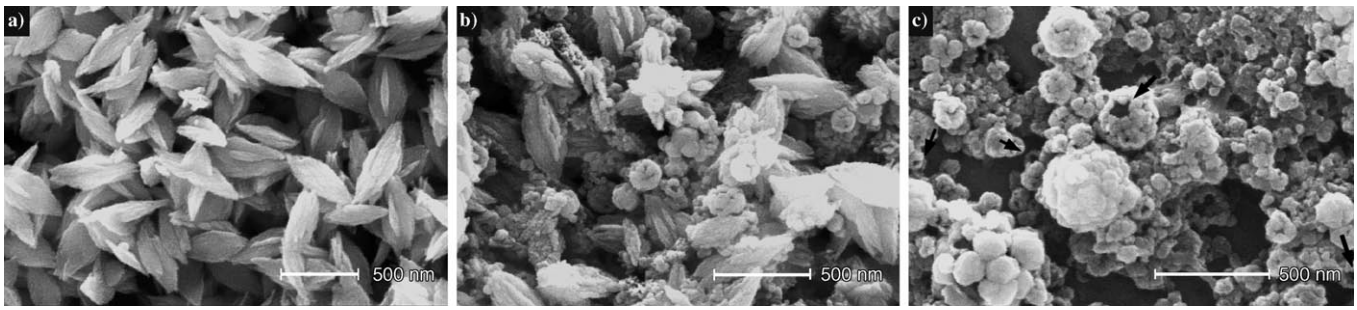

Figure 8. SEM images of CuO ellipsoidal formation with different surfactants: a) C_{18}TAB, b) C_{14}TAB, and c) C_{10}TAB. The arrows indicate the nanoshells.

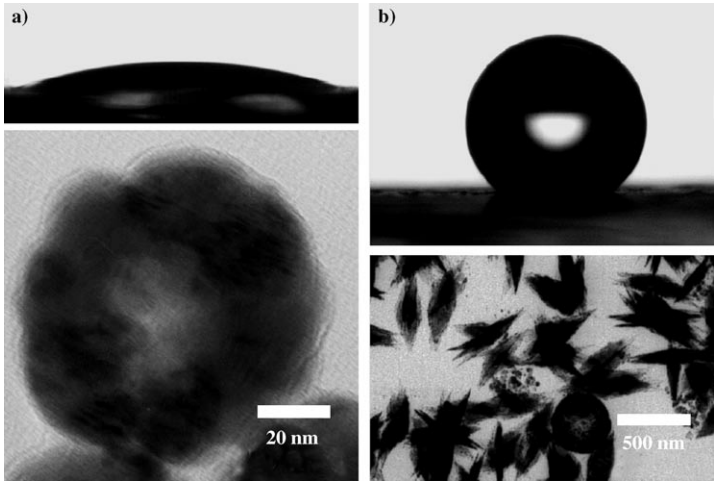

Figure 9. Shape of a water droplet on the surface of the a) Cu_2O nanoshells and b) CuO ellipsoids that were produced after 2 h reaction time.

bility changed from hydrophilicity to hydrophobicity as the Cu_2O nanoshells shifted to three-dimensional CuO aggregated ellipsoids. The enhanced hydrophobicity could be attributed to high surface roughness in CuO nanomaterials made of many aggregated nanoparticles.

Conclusion

We have demonstrated a surfactant-assisted hollowing reaction. The oxidative etching resulted in Cu_2O nanoshells. It was found that Cu_2O hollow nanospheres further converted into three-dimensional CuO ellipsoids by means of oxidation, fragmentation, and self-assembly processes. Interestingly, the CuO formation is strongly related to the surfactant length, whereby the longer surfactants favor the growth of the ellipsoidal structure. In addition, the as-synthesized Cu_2O and CuO nanomaterials reveal opposite natures of wettability. Overall, we have provided a new strategy to fabricate hollow nanostructures. Such a hollowing reaction with the aid of surfactants should have applications in the related corrosion–oxidation processes for other nanomaterials and different morphologies.

Experimental Section

Polydispersed copper nanoparticles were prepared by laser ablation of 0.02 g of CuO powders in 2-propanol (5 mL). An unfocused Nd:YAG laser (1064 nm) with laser fluence of 100 mJ/pulse was employed to irradiate mixtures containing CuO powders and 2-propanol for 5 min. This was followed by centrifugation to remove the remaining CuO powders. Subsequently, the prepared colloidal solutions were illuminated for an additional 5 min.[8,9]

For the synthesis of the hollow Cu_2O, 1 mL of Cu colloids in 2-propanol was injected into 4 mL of an aqueous solution of C_{16}TAB (cetyltrimethylammonium bromide), followed by reaction at 55 °C for 16 min. C_{16}TAB (2.2 mM) was predissolved in 4 mL of pure water. If the reaction time was extended to 4 h, the synthesized cuprous oxide (Cu_2O) nanoshells transformed into crystalline CuO ellipsoids. For the contact angle experiments, 20 mL of the as-prepared material, that is, hollow Cu_2O or ellipsoidal CuO, was washed in 2-propanol and allowed to settle on a $0.6 \times 0.6\ cm^2$ glass substrate, then dried in a vacuum.

Electron micrographs were obtained by using transmission electron microscopes (JEOL 3010 at 300 KV and PHILIPS CM-200 at 200 KV). A drop of the sample was placed on a copper mesh coated with an amorphous carbon film, followed by evaporation of the solvent in a vacuum desiccator. Scanning electron microscopy (SEM) images of the as-synthesized materials on the copper substrates were obtained by using a Hitachi S4200 field-emission scanning electron microscope. X-ray diffraction (XRD) results were collected by using a Rigaku D-Max IIIV diffractometer with $Cu_{K\alpha}$ radiation ($\lambda = 1.54056$ Å) at 30 kV and 30 mA. Contact angles (CA) were measured by using a contact-angle meter (OCA20, Dataphysics).

Acknowledgements

Funding from the National Science Council of Taiwan is gratefully acknowledged.

[1] a) J. Ghijsen, L. H. Tjeng, J. v. Elp, H. Eskes, J. Westerink, G. A. Sawatzky, *Phys. Rev. B* **1988**, *38*, 11322; b) T. Ito, H. Yamaguchi, T. Masumi, S. Aldachi, *J. Phys. Soc. Jpn.* **1998**, *67*, 3304; c) F. P. Koffyberg, F. A. Benko, *J. Appl. Phys.* **1982**, *53*, 1173; d) W. Shi, K. Lim, X. Liu, *J. Appl. Phys.* **1997**, *81*, 2822.
[2] a) J. B. Reitz, E. I. Solomon, *J. Am. Chem. Soc.* **1998**, *120*, 11467; b) J. A. Switzer, H. M. Kothari, P. Poizot, S. Nakanishi, E. W. Bohannan, *Nature* **2003**, *425*, 490; c) H. J. Cristau, P. P. Cellier, J. F. Spindler, M. Taillefer, *Chem. Eur. J.* **2004**, *10*, 5670.
[3] R. N. Briskman, *Sol. Energy Mater. Sol. Cells* **1992**, *27*, 361.
[4] a) J. Li, H. C. Zeng, *Angew. Chem.* **2005**, *117*, 4416; *Angew. Chem. Int. Ed.* **2005**, *44*, 4342; b) D. G. Shchukin, G. B. Shchukin, H. Möhwald, *Angew. Chem.* **2003**, *115*, 4610; *Angew. Chem. Int. Ed.* **2003**, *42*, 4472; c) Y. Sun, Y. Xia, *Anal. Chem.* **2002**, *74*, 5297; d) X. L. Li, T. J. Lou, X. M. Sun, Y. D. Li, *Inorg. Chem.* **2004**, *43*, 5442.
[5] a) T. Ung, L. M. Liz-Mazán, P. Mulvaney, *Langmuir* **1998**, *14*, 3740; b) F. Caruso, A. Caruso, H. Möhwald, *Science* **1998**, *282*, 1111.
[6] a) Y. Yin, R. M. Rioux, C. K. Erdonmez, S. Hughes, G. A. Somorjai, A. P. Alivisatos, *Science* **2004**, *304*, 711; b) Y. Chang, M. L. Lye, H. C. Zeng, *Langmuir* **2005**, *21*, 3746.
[7] Y. Chang, J. J. Teo, H. C. Zeng, *Langmuir* **2005**, *21*, 1074.
[8] M. T. Hsiao, S. F. Chen, D. B. Shieh, C. S. Yeh, *J. Phys. Chem. B* **2006**, *110*, 205.
[9] a) M. S. Yeh, Y. S. Yang, Y. P. Lee, H. F. Lee, Y. H. Yeh, C. S. Yeh, *J. Phys. Chem. B* **1999**, *103*, 6851; b) T. Y. Chen, S. F. Chen, H. S. Sheu, C. S. Yeh, *J. Phys. Chem. B* **2002**, *106*, 9717.
[10] a) A. C. Curtis, D. G. Duff, P. P. Edwards, D. A. Jefferson, B. F. G. Johnson, A. I. Kirkland, A. S. Wallace, *J Phys. Chem.* **1988**, *92*, 2270; b) Z. Liu, Y. Yang, J. Liang, Z. Hu, S. Li, S. Peng, Y. Qian, *J. Phys. Chem. B* **2003**, *107*, 12658.
[11] M. Yin, C. K. Wu, Y. Lou, C. B. Burda, J. T. Koberstein, Y. Zhu, S. O'Brien, *J. Am. Chem. Soc.* **2005**, *127*, 9506.
[12] K. Borgohain, N. Murase, S. Mahamuni, *J. Appl. Phys.* **2002**, *92*, 1292.
[13] H. Zhou, W. Cai, L. Zhang, *Appl. Phys. Lett.* **1999**, *75*, 495.
[14] M. G. Fontana, N. D. Greene, *Corrosion Engineering*, 2nd ed., McGraw-Hill, **1978**, pp. 41–52.
[15] G. Nagy, D. Roy, *Langmuir* **1993**, *9*, 1868.
[16] C. I. Elsner, R. C. Salvarezza, A. Arvia, *Electrochim. Acta* **1988**, *33*, 1735.
[17] J. Rodríguez-Fernández, J. Pérez-Juste, P. Mulvaney, L. M. Liz-Marzán, *J. Phys. Chem. B* **2005**, *109*, 14257.
[18] Z. Zhang, H. Sun, X. Shao, D. Li, H. Yu, M. Han, *Adv. Mater.* **2005**, *17*, 42.
[19] L. Feng, S. Li, Y. Li, H. Li, L. Zhang, J. Z. Y. Song, B. Liu, L. Jiang, D. Zhu, *Adv. Mater.* **2002**, *14*, 1857.

Received: November 30, 2005
Published online: March 10, 2006

